17th World Conference on Earthquake Engineering, 17WCEE

Sendai, Japan - September 13th to 18th 2020

ROTATIONAL STIFFNESS OF BENDING MOMENT RESISTING SLABS INSTALLED IN BUILDINGS WITHOUT FOUNDATION GIRDERS

N. Munakata[(1)], Y. Michishita[(2)], H. Miyasaka[(3)], K. Yamagishi[(4)]

[(1)] *Graduate student, Kanazawa Institute of Technology, b1619490@planet.kanazawa-it.ac.jp*
[(2)] *Former Graduate student, Kanazawa Institute of Technology, b6801692@planet.kanazawa-it.ac.jp*
[(3)] *Director, Miyasaka Architect Office Corporation, arch-eng@miyasaka-office.jp*
[(4)] *Professor, Kanazawa Institute of Technology, kuniaki@neptune.kanazawa-it.ac.jp*

Abstract

In recent years, the construction of buildings without foundation girders has becoming increasingly important from the perspective of environmental protection. Foundation girders play an important structural role in resisting the bending moment generated in the column base and distributing some of the axial force to the other piles. However, the members comprising a foundation girder are larger than those forming the superstructure so need to be built underground; this not only requires a lot of building materials, but also generates a lot of waste soil, which is detrimental to the environment. Thus, buildings without foundation girders are more environmentally friendly and boast shorter construction times, which is highly advantageous for business owners wishing to use the buildings. However, the lack of members able to resist the bending moment at column bases can lead to increased displacement during an earthquake. Therefore, we proposed a method for reducing displacement that does not require special devices or materials. This method employs "bending moment resisting slabs" connected to the column base, which are buried in ground improved by cement injection. The purpose of this study was to calculate the rotational stiffness of the "moment resisting slab" by finite element model (FEM) analysis. The building for the analysis was a steel structure with a steel pipe pile. We assumed a single-layer steel structure with a span of 10 m and a floor height of 5 m. The pile head consists of a pile cap and a moment resisting slab, and the surrounding ground near the pile cap was improved by cement slurry injection. The rotational stiffness of the moment resisting slab was calculated by applying a concentrated moment to the column base. The parameters include the size of the pile cap and the degree of ground improvement. The analysis also considered slab lift due to rotation of the foundation. The results indicated that the maximum effective radius of the moment resisting slab was 2 m, the improved ground greatly contributed to the rotational resistance, and the pile had a substantial influence on the rotational resistance. Renovation and retrofitting of existing buildings are preferable when prioritizing environmental protection; however, in earthquake-prone countries, reconstruction is necessary for buildings with reduced seismic performance due to aging. Specifically, buildings without foundation girders, which are easy to dismantle, are important for stimulating modern architecture in societies with a rapidly changing economic situation. This study provides an important basis for solving problems related to buildings without foundation girders.

Keywords: Buildings without foundation girders; Moment resisting slab; Rotational stiffness; Axisymmetric model

1. Introduction

In construction, the foundation is a key component supporting the building; it should be constructed rigidly in order to reliably transmit the weight and inertial force of the superstructure to the supporting ground through footings or piles. However, in recent years, buildings without foundation girders (hereafter referred to as NF_GBs; i.e., Non-Footing Girder Buildings) have been constructed for relatively small-scale production and commercial facilities [1, 2]. As shown in Fig. 1(a), the foundation of a building with a general foundation girder (hereafter referred to as F_GB) consists of a foundation girder, a pile cap, a pile, and an anchor bolt, all of which are rigidly connected. On the other hand, as shown in Fig. 1(b), the foundation of NF_GBs is constructed by directly connecting both flanges of the steel pipe columns and steel pipe piles with high-strength bolts, eliminating the need for foundation girders and anchor bolts [1]. Therefore, an NF_GB is expected to have

a shorter construction period and significantly reduced construction costs. These advantages are significant from an environmental design perspective [3].

A pioneering example of an NF_GB is a station building above a railway track. As the railroad track exists at the foundation level, a foundation girder cannot be physically constructed orthogonal to the track. The NF_GB was first considered by Takei et al. [4]; in 1987, the first NF_GB structural design standard was published for low-rise buildings above railway tracks in Japan. It is known that the interstory drift of an NF_GB during an earthquake tends to be larger than that of an F_GB [5, 6]. Moreover, when designing small-scale buildings in Japan, an allowable stress design is often applied; i.e., a design that only considers the stress generated in the frame and not the deformation of the building [7]. Therefore, a small-scale building in which only the allowable stress design is applied may exhibit large deformation in the event of a large earthquake [5]. Considering the damage of exterior materials such as sashes and exterior finishing materials like an autoclaved lightweight aerated concrete panel, as well as the reusability of the building after the earthquake, it is necessary to devise countermeasures to reduce the displacement response of NF_GBs to a similar level as that of general buildings.

Michishita and Yamagishi [8] conducted a seismic response analysis of a one-story lightweight S-structure and determined the relationship between the flexural rigidity of the foundation girder and the interstory drift of the superstructure. The design of foundation girders varies because it is based on engineering judgments of the construction costs and building grade determined by the structural designer. However, when considering the general dimensions of a frame member, foundation girders typically exhibit flexibility and do not become completely rigid [8]. Therefore, this study proposes a method for transmitting the bending resistance of a general flexible foundation girder to the foundation of an NF_GB.

This study focuses on an earthen floor slab supporting the first floor of a building; the method for resisting the bending moment generated on the column base employs the bearing of the earthen floor structural slab connected to the column. In order to determine the basic characteristics related to the rotational stiffness of the proposed moment resisting slab, the outline of the slab is first introduced. Then, a finite element model (FEM) is proposed using axisymmetric elements to construct the moment resisting slab. The effect of the dimensions of each part of the proposed slab on the rotational stiffness is discussed. However, the axisymmetric element involves elastic analysis; thus, it is not possible to simulate separation between the slab and the ground when the bending moment generated in the column base acts on the center of the slab as an external force. Therefore, a 3D model that can consider slab separation from the ground for the same model is constructed, and the difference in rotational rigidity between the axisymmetric element model and the 3D model is discussed.

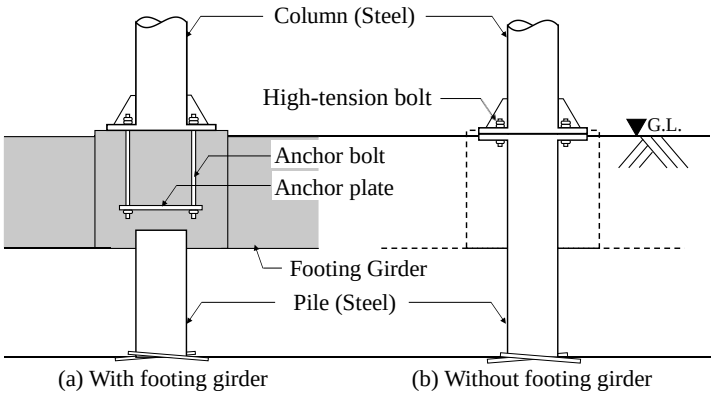

Fig. 1 – Detail of a pile-column joint and location of the expansion joint

2. Outline of the column-pile connection with the earthen floor slab

Fig. 1 (a) shows a conceptual diagram of the NF_GB. The columns and piles are steel pipes, and both are connected by high-strength bolts via a base plate and cast concrete to form the pile caps. Part of the earthen floor slab and the pile cap are integrated, and an expansion joint is installed at a certain distance from the

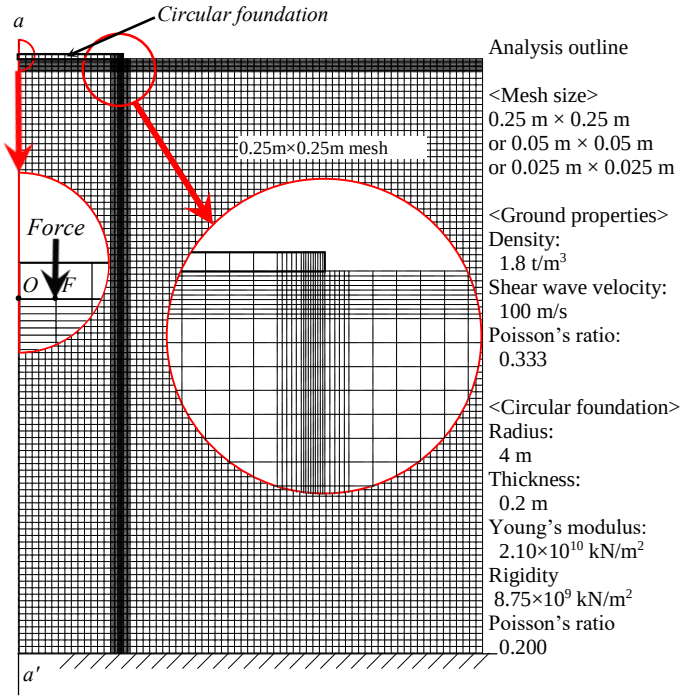

Fig. 2 – Analysis model (axisymmetric model)

column. As shown in Fig. 1 (b), the plane shape of the expansion joint is rectangular (or square) according to the concrete setting workability. The earthen floor slab integrated with the columns and piles and surrounded by the expansion joint is termed the moment resisting slab in this study. In addition, considering the ground characteristics of the site and the workability of the building, it is assumed that soil improvement is applied directly below the moment resisting slab.

3. Analysis model and accuracy verification

3.1 Accuracy of the analysis model

The purpose of this study is to understand the basic characteristics of the static rotational stiffness of the moment resisting slab with respect to the sizes of the slab parts and the soil improvement area. Therefore, the influence of each size is determined by conducting FEM analysis using the axisymmetric element, which is easy to calculate. Before conducting the parametric study, in order to examine the accuracy of the analysis, the static stiffness (rotational stiffness, K_R) (Eq. (1)) is simulated in the rotational direction of the circular rigid foundation on the ground surface using the research of Luco and Westmann [6].

$$K_R = \frac{8G_g {r_f}^3}{3(1-\nu_g)} \tag{1}$$

where G_g is the shear modulus of the ground, r_f is the radius of the circular foundation, and ν_g is the Poisson's ratio of the ground.

Fig. 2 shows the analysis model, assuming a ground with a depth of -22.75 m and a width of 17.75 m, with *a-a'* as the rotation axis. The soil density, ρ, is 1.8 t / m^2, the shear wave velocity, V_S, is 100 m / s, and the Poisson's ratio, ν_g, is 0.333. A circular foundation with a radius of r_s = 4m is set on this ground surface. Assuming that the circular foundation is a rigid foundation, a Young's modulus, E_f, of 2.10 × 10^{10} kN / m^2, which is 1,000 times that of concrete, is set for convenience. Regarding the other parameters, the plate thickness, t_f, is 0.2 m and the Poisson's ratio of the slab, ν_f, is 0.200. The mesh size is approximately 0.25 m

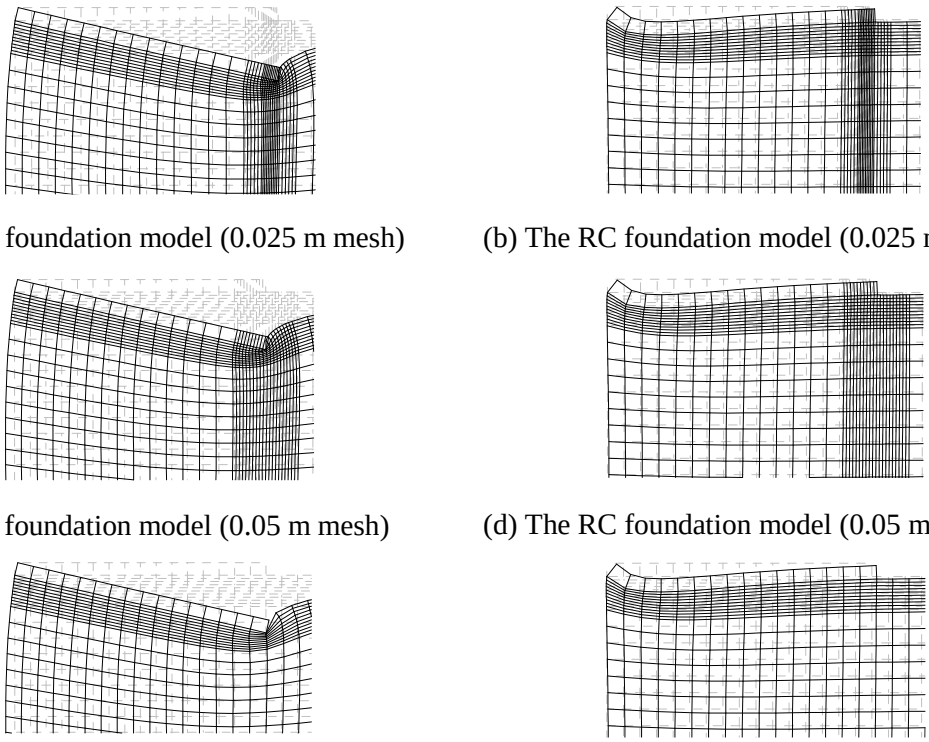

(a) The rigid foundation model (0.025 m mesh) (b) The RC foundation model (0.025 m mesh)

(c) The rigid foundation model (0.05 m mesh) (d) The RC foundation model (0.05 m mesh)

(e) The rigid foundation model (0.25 m mesh) (f) The RC foundation model (0.25 m mesh)

Fig. 3 – Deformation diagram for a minimum mesh size of (a, b) 0.025 m, (c, d) 0.05 m, and (e, f) 0.25 m. (a, c, and e) show the rigid foundation model and (b, d, and f) show the RC foundation model.

×0.25 m, and the edge of the rigid foundation where stress is concentrated is subdivided stepwise in the radial direction into 0.05-m and 0.025-m pitches. The boundary conditions are fixed only at the bottom, and the boundaries at the surface and sides are free. In addition, the displacement of point *O*, on which the external force acts in the radial direction (*r*-direction) and the depth direction (*z*-direction), is fixed. TDAP-III (ARC Information Systems) is employed for the analysis. The external force causes a concentrated moment to act on point *O* in Fig. 2. However, as TDAP-III cannot directly input the concentrated moment, an equivalent *z*-direction force applied to point *F*. The concentrated moment is 10 kNm.

Fig. 3(a) shows a deformation diagram of the rigid foundation, in which the circular foundation rotates almost rigidly around point *O*. The rotational stiffness, calculated by dividing the applied concentrated moment by the rotation angle about point *O*, is 4.579×10^6 kNm / rad. The rotational stiffness calculated from Eq. (1) is 4.606×10^6 kNm / rad, resulting in an error of 0.586%; i.e., there is approximate agreement with the theoretical value. However, there is a possibility that the analysis model described later in this manuscript cannot be constructed due to computational capacity limitations. Therefore, the rotational rigidity error for an increased mesh size of the edge part in the *r*-direction is examined. Fig. 3(c) and (e) show the rigid foundation deformation when the mesh size around the edge in the *r*-direction is 0.05 m and 0.25 m, respectively. The corresponding rotational stiffness values are 4.577×10^6 and 4.685×10^6 kNm / rad, and the errors with respect to Fig. 3 (a) are 0.0560% and 2.318%, respectively. However, these errors are attributable to the increase in stress at the edge due to the rigid foundation assumption. In a soft foundation, an increase in stress at the edge will be less likely to occur.

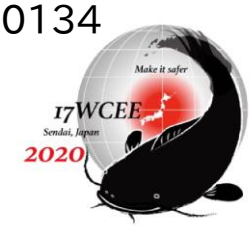

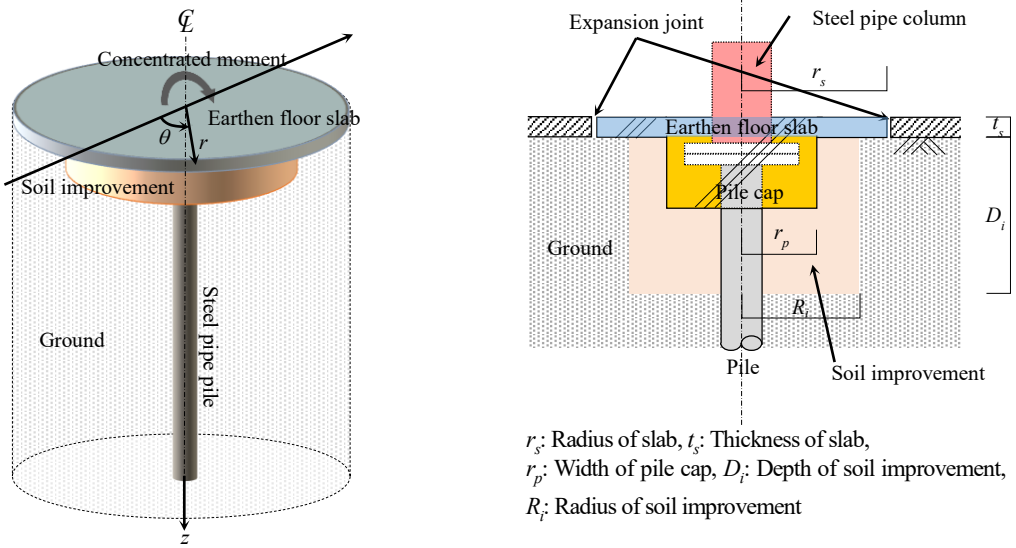

(a) Isometric view (b) Cross-section of the moment resisting slab

Fig. 4 – (a) Isometric view and (b) cross-section of the moment resisting slab

The rotational stiffness for an RC foundation structure is also calculated using the analysis model of the three mesh sizes around the edge in the *r*-direction. The properties are the same as in Fig. 2 except that the Young's modulus of the circular foundation is set to the RC Young's modulus E_c = 2.10 × 10^7 kN / m^2. Fig. 3(b), (d), and (f) show the deformation diagrams of the RC foundation when the mesh size of the edge part is varied. Ground deformation at the edge is smaller than that in Fig. 3(a), (c), and (e). In other words, the stress concentration at the edge is mitigated. On the other hand, the bending deformation of the RC foundation near the rotation axis is increased due to the Young's modulus of 1/1000. The rotational stiffness values calculated from the deformation results in Fig. 3(a), (c), and (e) are 1.182 × 10^6 kNm / rad, 1.180 × 10^6 kNm / rad, and 1.180 × 10^6 kNm / rad, respectively. The difference between Fig. 3(b) and (f) is 0.169%. Thus, to calculating the rotational stiffness for the RC foundation, we employ a minimum mesh size of the edge part of 0.05 m.

3.2 Moment resisting slab analysis model

Fig. 4 shows a schematic diagram of the moment resisting slab. To understand only the rotational stiffness of the foundation, an analytical model without a superstructure is constructed. The moment resisting slab, soil improvement part, and pile are configured as shown in Fig. 4(a); a cross-sectional view is shown in Fig. 4(b). Table 1 shows the analysis parameters, which are the radius r_s of the moment resisting slab (r_s), the thickness of the slab (t_s), the radius of the pile cap (r_p), and the soil improvement range (depth D_i, radius (width) R_i). The single underlined values shown in Table 1 are reference values, and double underlined values are the reference values when the soil improvement parameters D_i and R_i are used.

The properties of the moment resisting slab and the pile cap are those of RC, and soil improvement is assumed to involve a high-strength cement-based improved soil [7] with a density of 1.8 t / m^3 and a shear wave speed of 1,000 m / s. A steel pipe pile with a Poisson's ratio of 0.333, a pile of 300 mm, and a thickness of 15.7 mm is replaced with an equivalent single material with a radius of 150 mm, including sandy soil with a density of 4.33 t / m^3 and a Young's modulus of 1.37 × 10^8 kN / m^2. The Poisson's ratio is 0.333. In order to calculate the rotation angle of the pile head, the Young's modulus of the pile head is set to 1000 times that of concrete, and the pile head is assumed to be rigid (Fig. 5: Rigid element).

Table 1 – Analysis parameters (m)

No.	Parameter	Values
(1)	Radius of slab r_s	1.0, 2.0, 3.0, 4.0
(2)	Thickness of slab t_s	0.15, 0.18, 0.20, 0.25
(3)	Radius of pile cap r_p	0.50, 1.0, 1.5, 2.0, 2.5
(4)	Depth of soil improvement D_i	0.0, 1.0, 1.5, 2.0, 4.0
(5)	Radius of soil improvement R_i	0.0, 1.0, 2.0, 3.0, 4.0

*Single underlined values are basic parameters for (1)-(3), double for (4), (5)

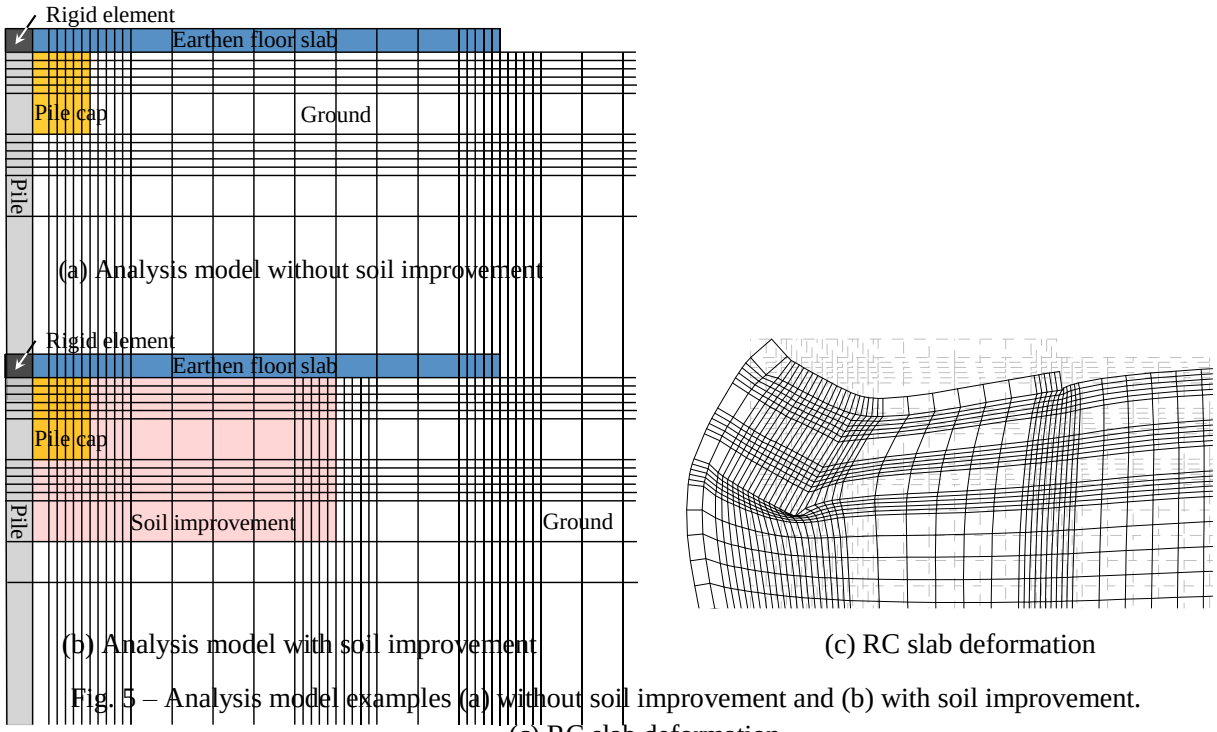

Fig. 5 – Analysis model examples (a) without soil improvement and (b) with soil improvement. (c) RC slab deformation

Fig. 5(a) and (b) show an enlarged view of the slab of the analysis model both with and without soil improvement. Fig. 5(c) shows an example of slab deformation when the slab radius is r_s = 3 m, the slab thickness is t_s = 0.18 m, the pile cap radius is r_p = 1 m, the depth of the ground improvement is D_i = 1 m, and the radius is R_i = 2 m. It is clear that the strain is concentrated at the ends of the pile cap and the slab. The pile cap covers the joint between the pile and the column. Increasing the radius of the pile cap increases K_R; thus, increasing the pile cap increases the size of the base member and is incompatible with the NF_GB design concept. Instead, K_R can be increased by improving the soil directly below the slab. Soil improvement with a radius of 3 m can achieve a larger K_R than a pile cap with a radius of 2.5 m. The soil assumed in this study is harder than that of general soil improvement. Although the hardness of the improved soil does not need to be as high as RC, this can increase the K_R value. Moreover, K_R is proportional to the thickness of the slab and the radius of the slab that will result in an increase in K_R is limited.

3.3 Influence of bending resistance slab dimensions on rotational stiffness

Fig. 6 shows the change in rotational stiffness, K_R, for each parameter. Each figure also shows the K_R without a pile. According to the slab radius, r_s (at a slab thickness of 0.18 m), the change in K_R is small when the radius is 2 m or more, and increasing r_s is not expected to increase K_R (a). According to the slab thickness, t_s (at a slab radius of 3 m), K_R increases almost in proportion to t_s (b). According to the pile cap width (radius) r_p (at a slab radius and thickness of 3 m and 0.18 m, respectively), K_R increases in accordance with r_p, but the rate of increase of K_R slows down after r_p exceeds 2 m (c). According to the depth of ground improvement, D_i

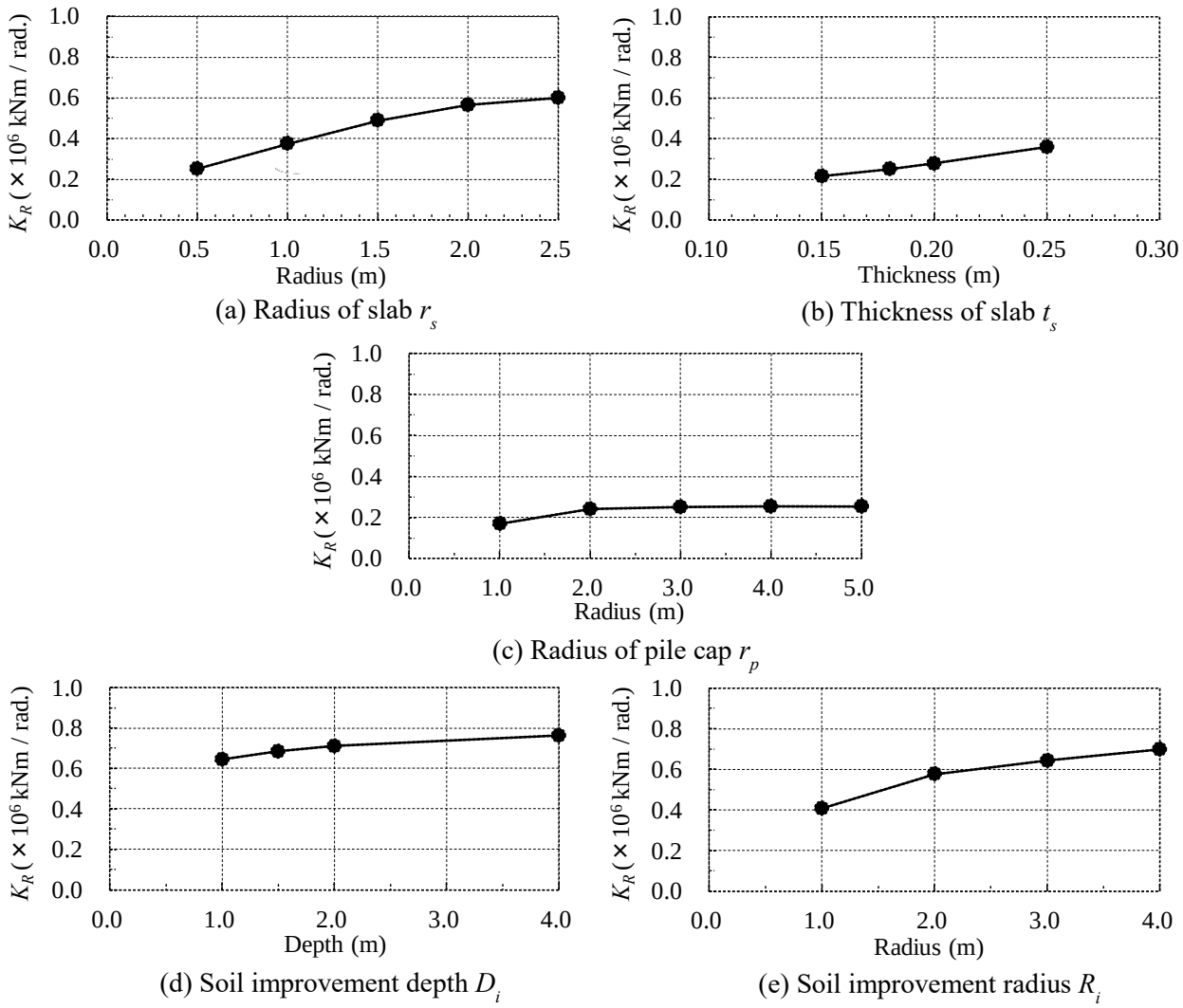

(a) Radius of slab r_s
(b) Thickness of slab t_s
(c) Radius of pile cap r_p
(d) Soil improvement depth D_i
(e) Soil improvement radius R_i

Fig. 6 – Rotational stiffness for each parameter

(improvement width R_i = 3.0 m), the K_R increases slightly with an increase of D_i, but no remarkable change is observed (d). Finally, according to the width, R_i (improvement depth D_i = 1.0 m) of the ground improvement body, K_R increases as R_i increases, but is almost saturated when R_i is 3.0 m or more (e).

The pile cap covers the joint between the pile and the column. Increasing the radius of the pile cap increases K_R; however, increasing the pile cap means increasing the size of the base member and is incompatible with the NF$_G$B design concept. Instead, K_R can be increased by improving the ground directly below the slab. Ground improvement with a radius of 3 m can achieve a larger K_R than a 2.5-m radius pile cap. Again, the ground is assumed to be harder than that for general ground improvement, which is unnecessary but means that the K_R can be increased with rigidity of the improved ground.

3.4 Rotational stiffness of each part of the moment resisting slab

As shown in section 3.3, the rotational stiffness changes depending on the dimensions of each part of the moment resistance slab. In this section, the rotational rigidity of each part of the slab is calculated, and the contribution of the moment resistance of each part is confirmed. Here, ground improvement is excluded. Fig. 7 shows the relationship between each parameter of the moment resistance slab (PCS) and the rotational stiffness shown in Fig. 6 . The rotational stiffness (CS) of the moment resistance slab with only the pile removed, with the pile only (P), with the pile cap only (C), and with the soil slab only (S) are all shown.

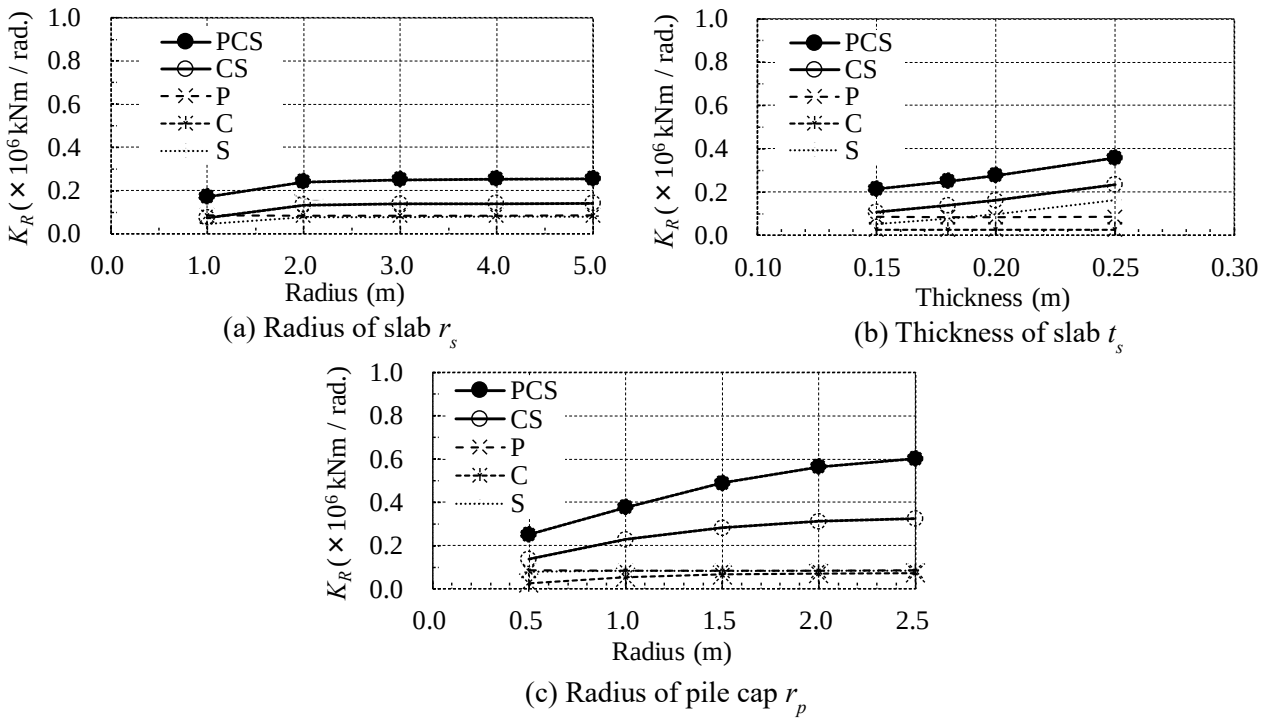

(a) Radius of slab r_s (b) Thickness of slab t_s

(c) Radius of pile cap r_p

Fig. 7 – K_R of PCS, CS, P, C, and S according to (a) Radius of slab r_s, (b) Thickness of slab t_s, and (c) Radius of pile cap r_p

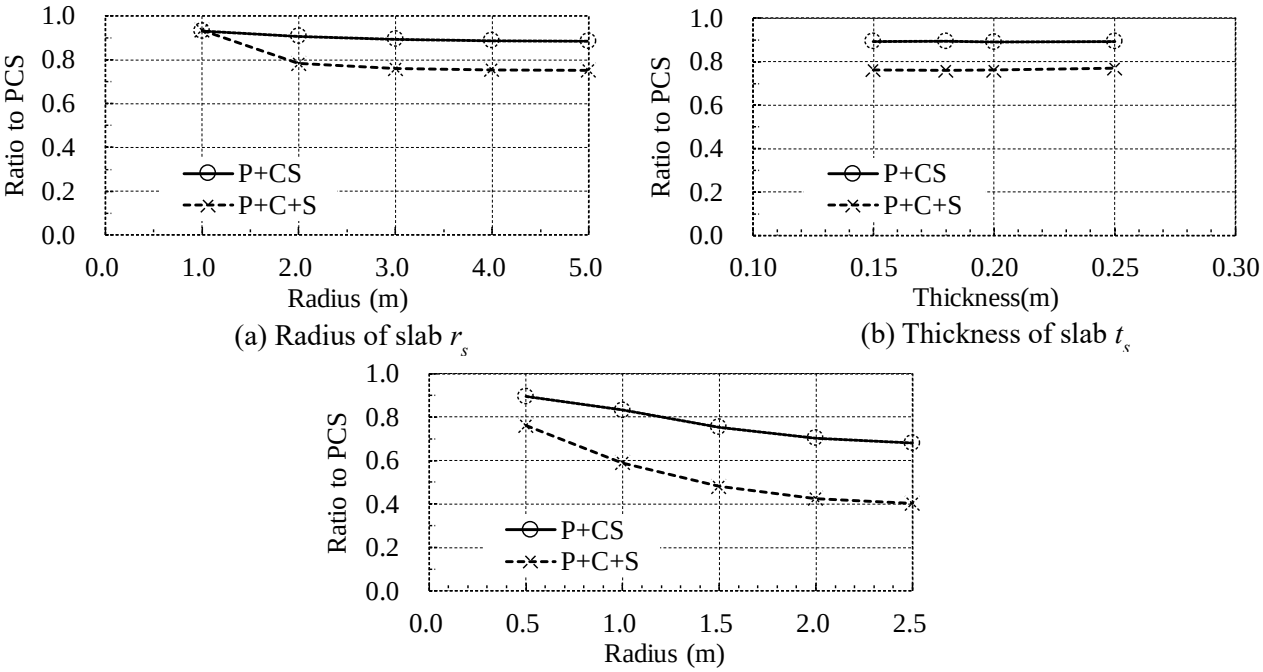

(a) Radius of slab r_s (b) Thickness of slab t_s

(c) Radius of pile cap r_p

Fig. 8 – Ratio of combined K_R to PCS according to (a) Radius of slab r_s, (b) Thickness of slab t_s, and (c) Radius of pile cap r_p

Regardless of the parameters, there is a remarkable difference between PCS and CS, indicating that the bending resistance of the pile in the moment resistance slab is large. At present, the NF_GB under consideration is based on a pile foundation (end-supported pile); however, it should be noted that, when directly constructing an NF_GB on a foundation, the rotational rigidity of the moment resistance slab is greatly reduced. However, the simple sum of CS and P has lower rotational rigidity than PCS. Fig. 8 shows the ratio of the sum of PSC and CS, the sum of CS and P, and the sum of P, C, and S. It can be seen that CS + P and C + S + P have lower rotational stiffness values than PCS for all parameters. Specifically, a remarkable decrease in the ratio occurs as the radius of the pile cap increases.

3.5 Relationship between flexural rigidity of the moment resisting slab and the foundation girder

The relationship between the rotational stiffness of the moment resisting slab and that of a generally installed foundation girder is determined in this section. Fig. 9 shows a plot of the rotational stiffness of the moment resisting slab described in section 3.3 for variable spans and section sizes of the foundation girders. The rotational stiffness obtained by the foundation girder is that when foundation girders of equal length are rigidly joined to the left and right of the column base and a unit moment is applied to the column base. The stiffness is obtained by a theoretical solution. The rotational stiffness of the moment resisting slab is arbitrarily plotted at a span of 10 m for convenience. H / b in the figure is the ratio (aspect ratio) between the height H and the width b of the foundation girder, where H is fixed at 0.5–2.0 m. For example, if H = 1.0 m and H / b = 2, b = 0.5 m. When the span is 10 m, the rotational stiffness calculated using the moment resisting slab exceeds the rotational stiffness of the foundation girder, H = 1.0 m, and the aspect ratio, H / b = 3. That is, depending on the device, the moment resisting slab has a rotational stiffness equivalent to that of a smaller foundation girder.

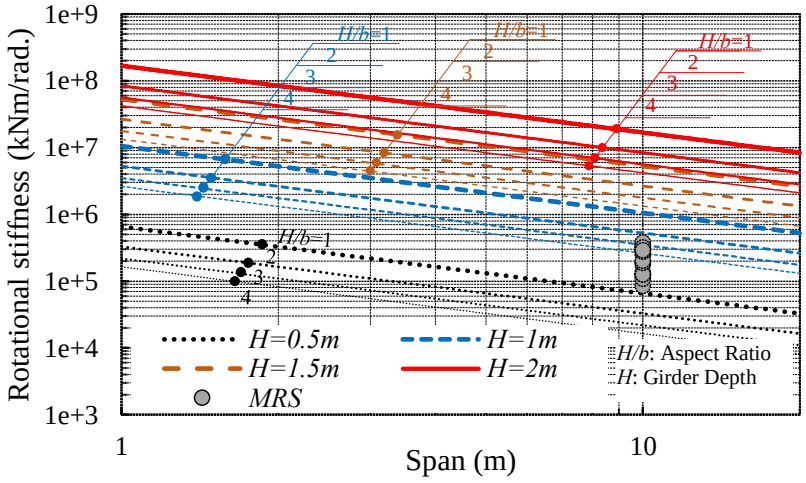

Fig. 9 – Relationship between girder span and rotational stiffness for a foundation girder including the proposed slab stiffness

4. Rotational rigidity considering slab and ground separation

4.1 Overview of the analysis model

To consider separation between the slab and the ground, it is necessary to construct an FE model. Although the target slab is the same as that in Fig. 4, a different FE model to that in Fig. 2 is constructed to reduce the calculation time. Fig. 10 shows the FE model for 3D analysis. The surrounding ground has been replaced with 32-direction SOLID elements that simulate an axisymmetric model, where the mesh size increases with

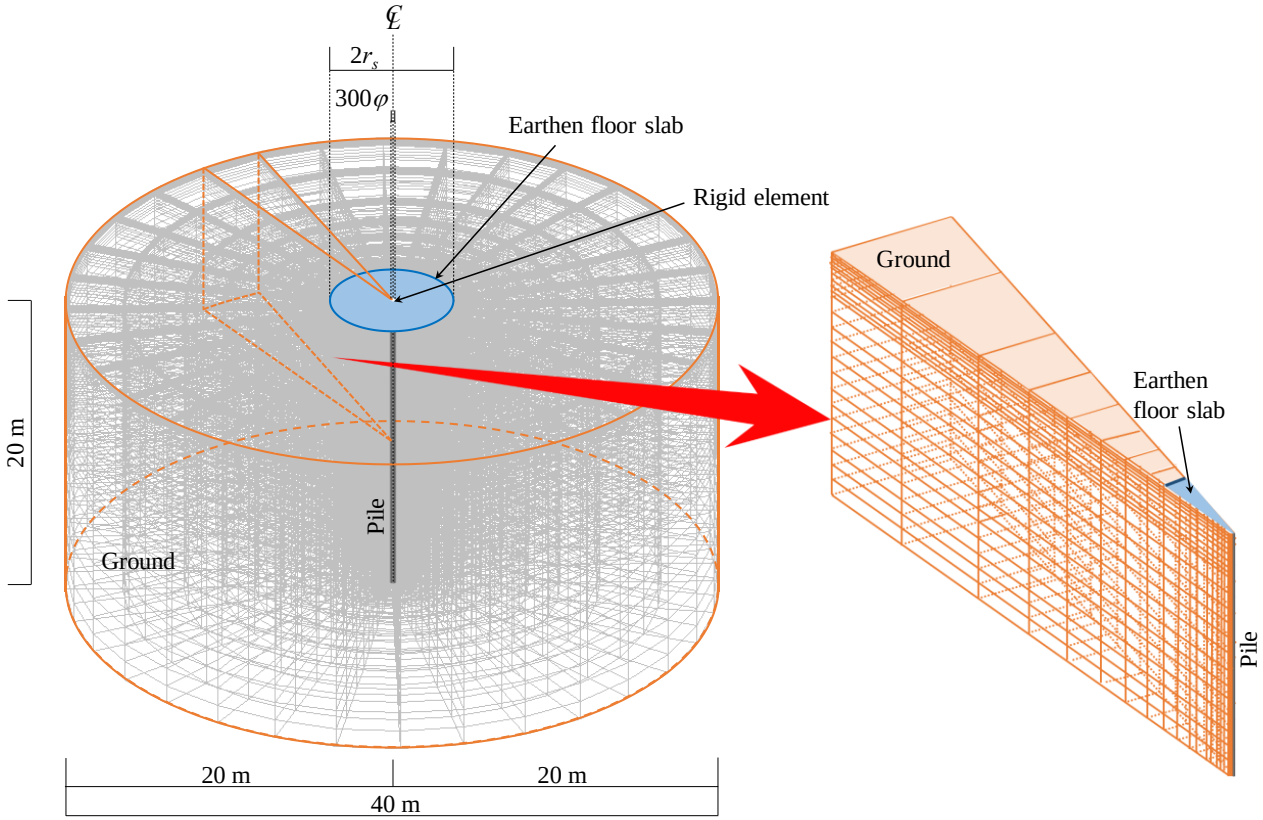

Fig. 10 – 3D model of the moment resisting slab

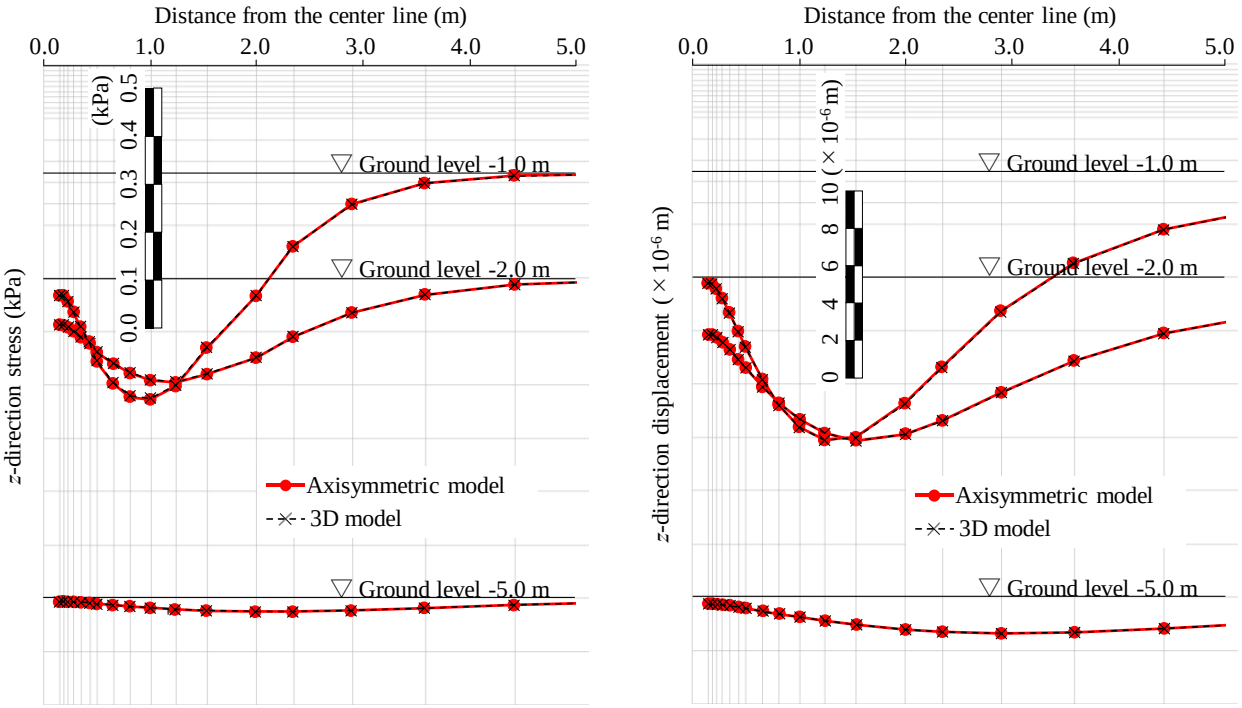

Fig. 11 – Confirmation of calculation accuracy of the 3D axisymmetric model

distance from the center. The element sizes of the soil slab, pile, pile cap, and ground improvement body are determined so as to be dependent on the ground mesh. The radius of the ground is set to 20 m, which is almost equal to the axisymmetric model. The pile is 300 mm in diameter and is replaced with SHELL elements, which is the same as the earthen floor slab. A rigid cap is placed on the pile head, and displacement of the pile head in the *z*-direction at GL-0m is caused only by rotation. A Joint element is used that exhibits high stiffness (0.250×10^6 kNm / rad.) when in contact with the ground and the soil slab and very low stiffness (0.147×10^6 kNm / rad.) when separated. The stress is transmitted to the ground and the soil slab only in the direction perpendicular to the slab, under the assumption of no in-plane shear stress.

As the meshing differs between the axisymmetric model and the 3D model, it is necessary to confirm the analysis accuracy when all elements are elastic. Fig. 11 shows the deformation diagram under the analysis conditions, which reveals good agreement between the analysis results of both models. The rotational rigidity K_R calculated by the models is 0.253×10^6 kNm / rad. and 0.252×10^6 kNm / rad., respectively, and the ratio between the two is 99.9%. Thus, the 3D model is used to evaluate the rotational rigidity considering deviation between the ground and the slab.

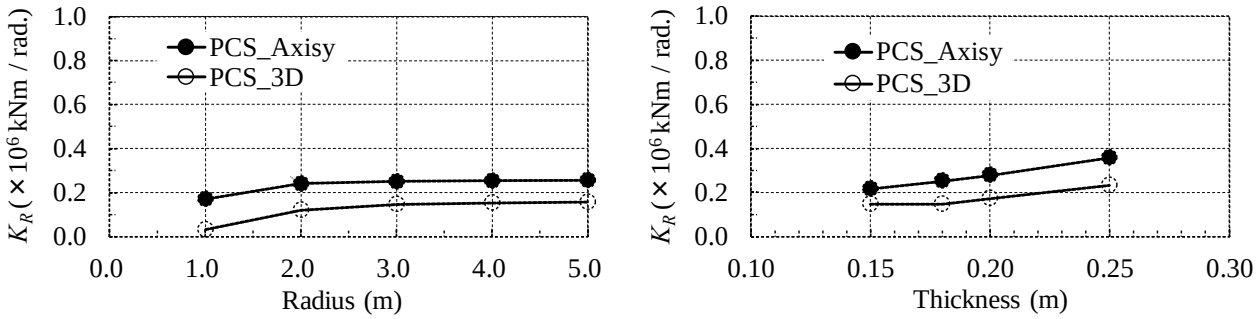

Fig. 12 – Comparison of K_R calculated by the axisymmetric model and the 3D model

4.2 Rotational rigidity considering slab and ground separation

Fig. 12 shows the difference between the axisymmetric model and the 3D model when varying the slab radius and thickness. As one side slab touches the ground and the other side detaches from the ground, the rotational stiffness, K_R, of the 3D model becomes less than that of the axisymmetric model. Although the K_R ratio between the 3D model and the axisymmetric model varies for the parameters, the K_R calculated by the 3D model is approximately half that calculated by the axisymmetric model. Therefore, if a moment resistance slab is incorporated into building design, the design should consider approximately half the rotational stiffness of the elastic analysis result.

5. Conclusions

This study focuses on soil slabs that are not generally treated as structural slabs for the purpose of reducing interlayer displacement in NF_GBs during earthquakes by combining soil slabs, pile caps, piles, and ground improvement bodies. A moment resisting slab was proposed and its rotational stiffness was evaluated using an axisymmetric model and a 3D model. The results indicated that not only the soil slab but also the pile greatly contributed to the rotational stiffness. In addition, the rotational stiffness can be increased at low cost by performing ground improvement directly below the earthen floor slab. However, the rotational rigidity obtained by the proposed slab is smaller than that obtained from the bending rigidity of a general foundation beam. Thus, a component that further increases the rotational rigidity should be developed in future research.

This study had some limitations. For example, we examined the rotational stiffness of a slab separated from a general earthen floor slab with an expansion joint. However, it is unfeasible to include an expansion joint inside earthen floor slabs because the slab would become uneven and water would be exuded directly below the slab over time. The earthen floor slab and the pile cap were modeled as circular shapes; however, a rectangular shape would be constructed in reality. There are many ways to further improve this research; for

example, by including a gap between the pile and the ground, considering frictional force between the pile, slab, and ground, analyzing the influence of nonlinearity of each component (particularly softening due to cracking of the RC slab), or by investigating the workability. Many challenges remain; therefore, future research should attempt to solve these issues.

6. Acknowledgments

The authors would like to express their gratitude to Y. Sawada, Professor Emeritus at Nagoya University, for the use of application TDAP-III, and S. Konda of the Kanazawa Institute of Technology for their helpful cooperation during the preparation of this report. In addition, we would like to thank Editage (www.editage.com) for English language editing.

7. References

[1] Sansei Inc. (n.d.): "ECS-TP" construction method, Retrieved January 30, 2020, from http://www.sansei-inc.co.jp/ecstp/ (in Japanese)

[2] JFE Civil Engineering & Construction Corp. (n.d.): "Ichi ichi" foundation construction method, Retrieved January 30, 2020, from https://www.jfe-civil.com/system/metalbuilding/ichiichi/ (in Japanese)

[3] Sakai K (2005): Environmental design for concrete structures. *Journal of Advanced Concrete Technology, Japan Concrete Institute*, **3** (1), 17-28.

[4] Takei Y, Yamada S, Hasuda T (2003): Structural design method for over-track low-rise buildings. *Quarterly Report of RTRI*, **60** (4), 166-173.

[5] Kobayashi T, Zou K, Nakano T, Miyamaoto Y (2016): Seismic response of a pile-supported building with no footing beam in shaking table test Part1: Outline of the shaking table test. *Summaries of Technical Papers of Annual Meeting Architectural Institute of Japan, Structures II*, 831-832. (in Japanese)

[6] Yamashita J, Miyasaka H, Yamagishi K (2017): Study on seismic behavior of non-footing girder building, Part 3: verification of modified penzien model and sectional force. *Summaries of Technical Papers of Annual Meeting Architectural Institute of Japan, Structures II*, 93-94. (in Japanese)

[7] Architectural Institute of Japan (2019): *AIJ Design standard for steel structures−based on allowable stress concept−(2005 Edition) English version.*

[8] Michishita Y, Yamagishi K, Miyasaka H, Miyamoto Y, Kobayashi T (2018): Study on nonlinear behavior of non-footing girder building. *The 12th International Symposium on Architectural Interchanges in Asia (ISAIA 2018)*, 639-642.

[9] Luco JE, Westmann RA (1971): Dynamic response of circular footings, *Journal of Engineering Mechanics*, **97** (EM5), 1381-1395.

[10] Sakamoto T, Asaka Y (2010): Shear wave velocity of cement treated–effect of fines content and dry density- . *Summaries of Technical Papers of Annual Meeting Architectural Institute of Japan, Structures I*, 467-468. (in Japanese)

